# Driving Bose-Einstein condensate vorticity with a rotating normal cloud

P. C. Haljan, I. Coddington, P. Engels, and E. A. Cornell*

*JILA, National Institute of Standards and Technology and Department of Physics,*
*University of Colorado, Boulder, Colorado 80309-0440*

(June 18, 2001)

We have developed an evaporative cooling technique that accelerates the circulation of an ultra-cold $^{87}$Rb gas, confined in a static harmonic potential. As a normal gas is evaporatively spun up and cooled below quantum degeneracy, it is found to nucleate vorticity in a Bose-Einstein condensate. Measurements of the condensate's aspect ratio and surface-wave excitations are consistent with effective rigid-body rotation. Rotation rates of up to 94% of the centrifugal limit are inferred. A threshold in the normal cloud's rotation is observed for the intrinsic nucleation of the first vortex. The threshold value lies below the prediction for a nucleation mechanism involving the excitation of surface-waves of the ground-state condensate.

03.75.Fi,67.90.+z,67.57.Fg,32.80.Pj

To paraphrase an ancient riddle, what happens when an irresistible torque meets an irrotational fluid? The answer has been known for more than 50 years: a quantized vortex is nucleated. Vortices alone contribute to a superfluid's rotation, so that the bulk of the fluid may remain curl-free. The nucleation of vortices in bulk superfluid Helium has been the topic of extensive study (for a review see [1]). In the archetypical experiment, a rotatable pot filled with a mixture of superfluid and normal liquid Helium undergoes gradual angular acceleration. The normal fluid and the walls of the pot rotate together as a rigid body, defining a rotating environment. At some threshold angular velocity, a vortex line is nucleated at the circumference of the pot, and then quickly migrates inward until it is collinear with the axis of rotation. Further angular acceleration results in the nucleation of more vortices; eventually the fluid is filled with an array of vortex lines [2]. A central theme [3] of this research is the question: to what extent is the nucleation process "extrinsic," *i.e.* dependent on such details as the roughness of the surface of the walls, and to what extent is it "intrinsic" [4,5], *i.e.* driven (in the limit of microscopically smooth walls) by the flow of normal fluid along the boundary of the superfluid? In the analogous rotating-potential experiments with a dilute-gas Bose-Einstein condensate (BEC), the confining potential and the normal fluid typically rotate at different rates [6]. In this context, the extrinsic-intrinsic question can be restated as: is it the confining potential or the normal fluid that defines the rotating environment?

Vortices in a BEC have been created with wavefunction engineering [7], through the decay of solitons [8,9], and in the wake of moving objects [10,11]. The first rotating-potential experiment to detect vortices in a BEC was performed by the Paris group [12]; results have also been obtained by the MIT [13] and Oxford [14] groups. In these experiments the role of the normal fluid was secondary to that of the rotating potential; it is conceivable the normal fluid was not rotating at all. This paper presents vortex nucleation experiments performed in the opposite limit, namely in the environment of a rotating normal gas in a static confining potential. Such an environment allows for the isolated study of the intrinsic mechanism for vortex nucleation.

Our experiments begin with a magnetically trapped cloud of about $6 \cdot 10^6$ $^{87}$Rb atoms, in the $|F = 1, m_F = -1\rangle$ hyperfine state, cooled close to the critical temperature $T_c = 67$ nK. The atoms are initially confined in an axially symmetric, oblate and harmonic potential [15] with axis of symmetry along the vertical ('z') axis. To induce rotation of the cloud, we first gradually apply an elliptical deformation to the potential in its horizontal plane of symmetry, and then rotate the deformation [16] about the vertical axis at a fixed angular frequency. The rotating potential is characterized by an axial frequency $\omega_z = 2\pi(13.6)$Hz, time-averaged radial frequency $\langle\omega_\rho\rangle = 2\pi(6.8)$Hz and a horizontal ellipticity of 25%. Such a large rotating trap asymmetry, accessible in the oblate configuration of our apparatus, is found to be necessary not only to get the cloud rotating, but also to sustain ongoing rotation. Moreover, in steady state the cloud does not reach the rotation rate of the applied asymmetry. We believe that the stirring process is fighting a small, static asymmetry that acts to despin the cloud [17].

In thermal equilibrium, a normal cloud rotates as a rigid body with the centrifugal force causing the cloud to bulge outwards in the radial direction. In order to detect the rotation, we use a nondestructive phase-contrast technique to image the cloud *in situ* from the side. Four sequential pictures of a given cloud are taken to average over oscillations in the widths and to improve the signal to noise. The cloud temperature is extracted from its vertical width $\sigma_z$, which is unaffected by rotation about the vertical axis. The rotation of the cloud $\Omega_N$ is determined from the aspect ratio, $\lambda = \sigma_z/\sigma_\rho$, using the relation:

$$\Omega/\omega_\rho = \sqrt{1 - (\lambda/\lambda_o)^2} \tag{1}$$

where $\lambda_o$ is the static aspect ratio. The technique of side-view imaging is crucial for distinguishing between changes in radial size due to temperature and to rotation.

For stirring rates up to 2.5 Hz, the rotation of the cloud reaches its steady-state value by 15 s or less. After 15 s, the rotating trap asymmetry is ramped off, leaving non-condensed clouds a factor of $1.2 - 1.3$ above $T_c$, for stirring frequencies $0 - 2.5$ Hz. Radio frequency (rf) evaporation is then used to cool the normal cloud to BEC. In the oblate configuration of our TOP trap [15], we have found that rf evaporation immediately quenches the rotation, presumably because the selection process, which removes atoms with large radial displacements, preferentially removes atoms with large axial components of their angular momentum. By adiabatically distorting the trap into a prolate geometry with $\{\omega_\rho, \omega_z\} = 2\pi\{8.35, 5.45\}$ Hz [18], we can instead cool the cloud by removing atoms with large *axial* displacements and thereby reduce the effect of the evaporation on the axial angular momentum. As the normal cloud is evaporated, its aspect ratio is observed to decrease continuously, indicating a monotonically increasing rotation rate (Fig. 1a). During the evaporation, the angular momentum per particle of the normal cloud remains roughly constant, even though the number of atoms is reduced by over a factor of five and temperature, by a factor of four (Fig. 1b). As the cloud cools and shrinks, it must spin up for the angular momentum per particle to remain fixed.

To reach significant rotation rates by the end of evaporation requires the lifetime of the normal cloud's angular momentum to be comparable to the evaporation time. The nearly one-dimensional nature of the evaporation together with the low average trap frequencies make cooling to BEC in the prolate trap very slow ($\sim$50 s). We obtain angular momentum lifetimes this long by shimming the azimuthal trap symmetry to better than 0.1%.

Towards the end of the evaporation, a condensate begins to appear at the center of the rotating normal cloud [19]. We discuss first the results of experiments in which we continue the evaporation until little or no normal fraction remains. In this case, we find that the rotating normal component has given birth to a condensate distended in its radial dimension, as one would expect for a classical rotating body under the influence of the centrifugal force. This effect is reminiscent of liquid Helium experiments, in which the surface of a rotating bucket of superfluid exhibits the same meniscus curvature as for an ordinary viscous fluid [20]. For large enough numbers of vortices in the condensate, the correspondence principle would suggest that the rotation field, coarse grained over the cloud, should go over to the classical limit of rigid-body rotation. In this limit, the classical Eq. (1) should connect condensate aspect ratio to rotation rate.

Alternatively, we can study the angular momentum in the BEC directly by exciting quadrupolar surface waves [21,22] with a rotating weak deformity of the magnetic
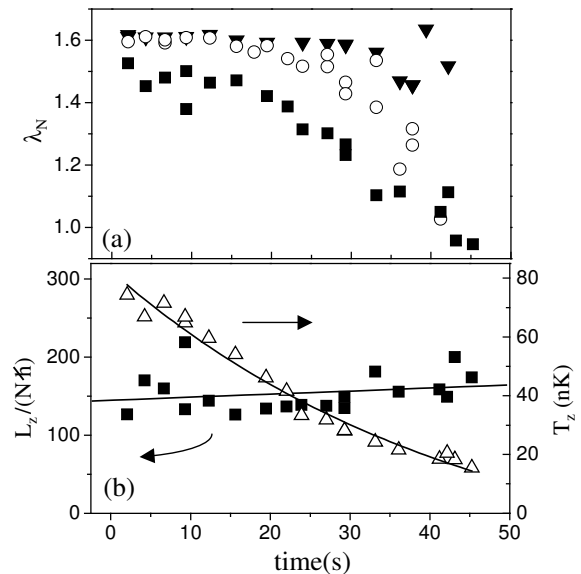


FIG. 1. (a)Aspect ratio of a rotating normal cloud during evaporation preferentially along the axis of rotation. Three different initial rotations of the cloud are shown, obtained by first stirring the cloud for 15s with an applied rotation rate of $0\omega_\rho$ (inverted triangles), $0.07\omega_\rho$ (open circles) and $0.37\omega_\rho$ (squares). (b)Angular momentum per particle (squares) and temperature (triangles) of the normal cloud during evaporation for the $0.37\omega_\rho$ case in (a).

trap. The quadrupolar surfaces waves are characterized by angular momentum quantum number $m_z = \pm 2$ where the $m_z = +(-)2$ excitation is taken to be co-(counter-)propagating with the rotation of the condensate. By varying the initial stir rate applied to the normal cloud, condensates of different aspect ratio can be accessed. In Fig. 2a, the frequency of the $m_z = \pm 2$ modes is shown as a function of condensate aspect ratio. The $m_z = +2$ mode is seen to speed up and the $m_z = -2$ to slow down due to the presence of vorticity in the condensate.

For small rotation rates, the splitting between the $m_z = \pm 2$ modes is predicted to be linearly proportional to the mean angular momentum of the condensate [23,24]. In the large-$\Omega$ limit of rigid-body rotation, Zambelli and Stringari [24,25] have used a sum-rule argument to show that the splitting between the modes is simply $2\Omega$, and, further, that the sum of the squared frequencies of the two modes is independent of rotation rate. A best fit of this model to the combined $m = \pm 2$ data is shown in Fig. 2a, where the rigid-body rotation rate has been inferred from the condensate aspect ratio and the classical Eq. (1). Perhaps more intuitively, the frequency splitting is plotted explicitly versus inferred rotation rate in Fig. 2b. The excellent agreement with the model of Zambelli and Stringari is compelling evidence in favor of the reasonableness of using Eq. (1) to connect the condensate aspect ratio with its effective rotation rate. This
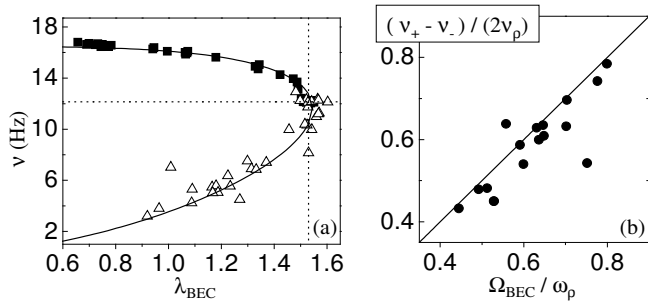
FIG. 2. Quadrupolar surface-wave spectroscopy of condensates formed in a rotating normal cloud. (a)Quadrupolar frequency as a function of condensate aspect ratio for the $m = +2$ (squares) and $m = -2$ (triangles) surface waves. Solid lines are a single fit to the combined data using the theory of Zambelli and Stringari [24,25]. Dotted lines indicate average frequency and aspect ratio for a static BEC. (b)The splitting between $m = \pm 2$ frequencies scaled by twice the trap frequency, plotted explicitly as a function of BEC rotation rate inferred from the aspect ratio. The solid line is the prediction from the same theory as in (a). Each plotted point is obtained from a single $m = -2$ measurement in (a) combined with a spline interpolation to the relatively quiet $m = +2$ data. Only aspect ratios smaller than 1.43 (corresponding to $\Omega_{BEC}/\omega_\rho \geq 0.35$) are included to avoid obtaining imaginary rotation frequencies due to experimental noise in the aspect ratio.

is further born out by extensive 3-D numerical simulations of the Gross-Pitaevskii equation for the parameters of our experiment, by Feder and Clark. Their numerical simulations confirm that a condensate in an environment rotating at frequency $\Omega > 0.5\,\omega_\rho$ will equilibrate close to the aspect ratio given by Eq. (1) [26].

In pure condensate samples we have observed aspect ratios as pronounced as $0.35\,\lambda_o$, corresponding to a rotation rate of $0.94\,\omega_\rho$. The rapid rotation rate, combined with the increased condensate area arising from its radial bulge, mean that the condensate must be supporting a large number of vortices. Feder and Clark [26] calculate 56. With these initial conditions, we have observed continued rotation for at least 140 s.

If the evaporation is stopped before the normal cloud has been completely removed, a comparison can be made between the aspect ratios, and hence rotation rates, of the condensate and normal cloud. By adjusting the initial stir rate applied to the normal cloud and the depth of the evaporation, we are able to reach different rotation rates for a given condensate fraction. After the evaporation is stopped, a time of 5 s is allowed for the gas to rethermalize to the last evaporative cut. We then take four nondestructive pictures and fit the images to a two-component distribution. Figure 3 shows a plot of the condensate aspect ratio $\lambda_{BEC}$ compared with the aspect ratio $\lambda_N$ of the normal cloud where each point represents a single realization of the experiment.
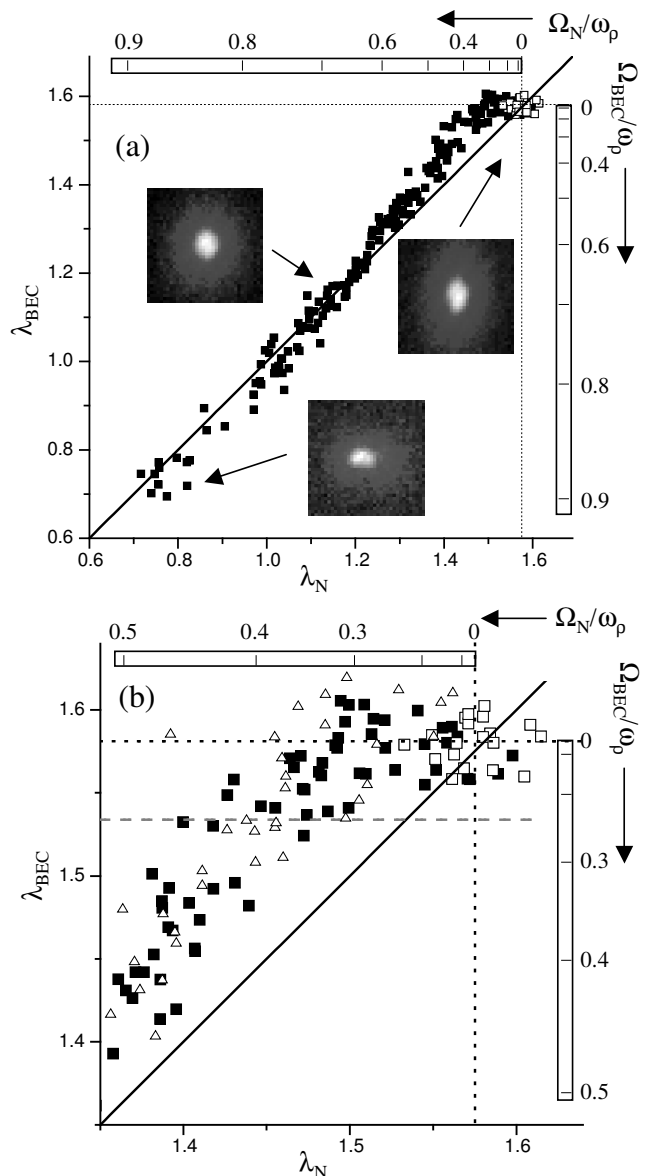


FIG. 3. (a)Aspect ratio of the BEC vs. that of the normal cloud after evaporation halted. Right and top scales provide a conversion from aspect ratio to classical rigid-body rotation rate for BEC and normal cloud respectively. Data for evaporation of both a static (empty squares) and rotating cloud (filled squares) are shown. Dotted lines indicate average static aspect ratios for both BEC and normal cloud. A solid 1:1 line is superimposed on the data. Three representative integrated density profiles of two-component clouds indicate the range of different aspect ratios observed. (b)A magnified version of the region of high aspect ratio (low rotation rate) in (a). Added to the plot are data (triangles) obtained with evaporative spin-up 3 times slower than for the filled squares. A dashed line indicates the aspect ratio expected for a BEC with a single, centered vortex as calculated by Feder and Clark [26].

For $\lambda_N < 1.36$ ($\Omega_N > 0.5\ \omega_\rho$), the condensate aspect ratio closely tracks the normal aspect ratio, providing a further manifestation of the correspondence principle for a highly rotating BEC. In the vicinity of $\lambda_N = 1.48$ ($\Omega_N = 0.35\ \omega_\rho$), we observe threshold behavior in the condensate rotation. At this low value of rotation we don't expect the rigid-body model to be valid for the condensate; but we make use of a numerical calculation by Feder and Clark [26] to indicate the change in condensate aspect ratio associated with the presence of a single, centered vortex (Fig. 3b). There is considerable scatter in the data so one cannot make a strong statement about the nature of the threshold shape, but clearly, somewhere between $0.32 < \Omega_N/\omega_\rho < 0.38$ the first vortex is nucleated.

A comparison of this threshold location with two theoretical rotation rates for our particular cloud provides some insight into the nature of the vortex nucleation. The first value is the threshold for the thermodynamic stability of a single vortex. For our experiment this number is $0.2 – 0.25\ \omega_\rho$ [27], distinctly lower than our observed threshold for nucleation. The second value is $\omega_{min}$, the frequency at which the slowest surface-wave mode propagates around the circumference of the condensate. The Paris group has shown that for their "extrinsic" nucleation process (vortices nucleated by a rotating asymmetric potential) the key mechanism is the non-linear excitation of surface waves [12,28]. Results from MIT [11,13] and from Oxford [14] are also consistent with such a mechanism. For the parameters of our experiment, $\omega_{min} = 0.4\ \omega_\rho$ [29]. Our observed threshold for "intrinsic" nucleation is clearly under this value, and thus we cannot interpret our effect in terms of a normal "wind" exciting surface waves on our condensate.

The data presented in Fig. 3 include a range of condensate fraction from 0.1-0.6 for each rotation rate of the normal cloud, although no segregation relative to either axis is evident for plots of different BEC fractions. Moreover, by reducing the rate of evaporation, we have decreased the rate of acceleration of the normal cloud rotation by a factor of 3, and still observe a threshold for vortex formation between 0.32 and 0.38 (Fig. 3b).

In future work we plan to use the controlled rotation of the normal cloud to study the life cycle of a BEC's vorticity [30], including any hysteresis between spin-up and spin-down due to vortex metastability. By halting the rotation of the normal cloud, we have already found that we can reduce the lifetime of the BEC's rotation by a factor of 10. Finally, the rotating normal cloud can create equilibrated condensates with very large rotation rates, which may allow us to approach the regime for which the vortices are so close-packed that their separation becomes comparable to the healing length [31].

*   Quantum Physics Division, National Institute of Standards and Technology.

[1] R. J. Donnelly, Quantized Vortices in Helium II, Cambridge University Press, Cambridge, UK (1991).

[2] V. K. Tkachenko, Zh. Eksp. Teor. Fiz. **50**, 1573 (1966) [Sov. Phys. JETP **23**, 1049 (1966)]; E. J. Yarmchuk, M. J. V. Gordon, and R. E. Packard, Phys. Rev. Lett. **43**, 214 (1979).

[3] V. M. H Ruutu, U. Parts, J. H. Koivuniemi, N. B. Kopnin, and M. Krusius, JLTP **107**, 93 (1997).

[4] J. S. Langer and M. E. Fisher, Phys. Rev. Lett. **19**, 560 (1967); S. V. Iordanskii, Zh. Exsp. Theor. Fiz. **48**, 708 (1965) [Sov. Phys. JETP **21**, 467 (1965).].

[5] E. Varoquaux, M. W. Meisel, and O. Avenel, Phys. Rev. Lett. **57**, 229 (1986); J.C. Davis *et al.*, Phys. Rev. Lett. **69**, 323 (1992).

[6] D. Guery-Odelin, Phys. Rev. A **62**, 033607 (2000).

[7] M. R. Matthews *et al.*, Phys. Rev. Lett. **83**, 2498 (1999); B. P. Anderson, P. C. Haljan, C. E. Wieman, and E. A. Cornell, Phys. Rev. Lett. **85**, 2857 (2000).

[8] B. P. Anderson *et al.*, Phys. Rev. Lett. **86**, 2926 (2001).

[9] Z. Dutton, M. Budde, C. Slowe and L.V. Hau, to be published.

[10] S. Inouye *et al.*, cond-mat/0104444.

[11] C. Raman *et al.*, condmat/0106235.

[12] K. W. Madison, F. Chevy, W. Wohlleben, and J. Dalibard, Phys. Rev. Lett. **84**, 806 (2000).

[13] J. R. Abo-Shaeer, C. Raman, J. M. Vogels and W. Ketterle, Science **292**, 476 (2001).

[14] E. Hodby *et al.*, condmat/0106262.

[15] W. Petrich, M. H. Anderson, J. R. Ensher, and E. A. Cornell, Phys. Rev. Lett. **74**, 3352 (1995).

[16] D. S. Jin *et al.*, Phys. Rev. Lett. **77**, 420 (1996).

[17] Small static trap asymmetries can have a disproportionately large effect compared to much larger rotating asymmetries. This is related to the fact (pointed out by Guery-Odelin [6]) that spin-up and spin-down times are very different for a given ($m = 2$) trap asymmetry.

[18] J. R. Ensher, Ph.D. thesis, University of Colorado (Boulder), 1998.

[19] In L.He. experiments, one expects very different behavior if one either (i) cools below $T_c$ before crossing the threshold rotation for vortex nucleation or (ii) vice versa. In our experiment, the harmonic "pot" means that case (i) applies: the new-born condensate is initially too small to support a vortex.

[20] D. V. Osborne, Proc. Phys. Soc. (London) **A63**, 909 (1950); R. Meservey, Phys. Rev. **133**, A1472 (1964).

[21] F. Chevy, K. W. Madison, and J. Dalibard, Phys. Rev. Lett. **85**, 2223 (2000).

[22] P. C. Haljan, B. P. Anderson, I. Coddington, and E. A. Cornell, Phys. Rev. Lett. **86**, 2922 (2001).

[23] S. Sinha, Phys. Rev. A **55**, 4325 (1997); R. J. Dodd, K. Burnett, M. Edwards, and C. W. Clark, Phys. Rev. A **56**, 587 (1997); A. A. Svidzinsky and A. L. Fetter, Phys. Rev. A **58**, 3168 (1998).

[24] F. Zambelli and S. Stringari, Phys. Rev. Lett. **81**, 1754 (1998).

[25] S. Stringari, private communication.

[26] D. L. Feder and C. W. Clark, unpublished.

[27] S. Sinha, Phys. Rev. A **55**, 4235 (1997), E. Lundh. C. J. Pethick, and H. Smith, Phys. Rev. A **55**, 2126 (1997), Y. Castin and R. Dum, Eur. Phys. J. D **7**, 399 (1999).

[28] K. W. Madison, F. Chevy, V. Bretin, and J. Dalibard, Phys. Rev. Lett. **86**, 4443 (2001).

[29] F. Dalfovo and S. Stringari, Phys. Rev. A **63**, 011601 (R) (2000).

[30] P. O. Fedichev and A. E. Muryshev, cond-mat/0004264.

[31] Tin-Lun Ho, cond-mat/0104522.